

A channel preemption model for vertical handoff in a WLAN-embedded cellular network

Tsang-Ling Sheu · Wei-Feng Wei

Published online: 11 April 2009
© Springer Science+Business Media, LLC 2009

Abstract In this paper, a channel preemption model for vertical handoff in a WLAN-embedded cellular network is presented. In a heterogeneous networking environment, since many wireless LANs may be deployed within the coverage of a cellular network, horizontal handoffs among neighboring WLANs and vertical handoffs between a WLAN and the cellular network could occur frequently. Performance in terms of blocking probability of the cellular network can be seriously degraded if the channels are not appropriately allocated. The novelty of this paper is right in that a newly initiated mobile node (MN) outside the WLAN coverage can preempt the channels occupied by an MN inside the WLAN coverage when the cellular channels are completely used up. The channel preempted MN is forced to switch its network access to a WLAN. This proposed channel preemption scheme can effectively reduce the blocking probability while not disrupting any of the existing connections within WLANs. For the purpose of performance evaluation, we build a three-dimension Markov chains to analyze the proposed channel preemption mechanism. We derive the equations of move-in and move-out mobility rates based on the node speed and residence times, respectively. The network performance in terms of the number of active WLAN users, the channel utilization and the channel blocking probability of a cellular network, the preemption probability, and the preempted probability of an MN are calculated. From the analytical results, we observe the performance improvements by varying the node speed and the ratio of WLAN coverage.

Keywords WLAN · Cellular networks · Blocking probability · Vertical handoff · Channel preemption · Markov chains · Mobility

1 Introduction

With the advent of wireless communication technologies, various multimedia applications in traditional wired networks have been migrated into portable devices. Many previous works have pointed out the integration of wireless LANs (WLAN or IEEE802.11 b/g/a) and 3G/4G cellular systems can substantially improve the utilization of wireless resources, such as bandwidth. However, in this heterogeneous networking environment, frequent handoffs could occur between any two WLANs or between a WLAN and a cellular network. The overall performance may be seriously degraded due to frequent handoffs if network resources are not appropriately allocated.

Previous works on channel preemption models were mostly focused on a homogeneous network. Chen and Wu [1] proposed a scheme for cellular networks that can dynamically adjust the voice-call blocking probability to maintain the transmission quality of data traffic. By embedding the channel preemption scheme, Ahma et al. [2] proposed a prediction methodology to maximize the user satisfaction. Das et al. [3] tried to balance between the number of mobile users and the user satisfaction in a wireless environment. In [4, 5], a multi-mode channel preemption mechanism was proposed for CDMA systems to guarantee the fairness of different mobile users. In order not to reduce the overall system throughput, Kim et al. [6, 7] presented a channel preemptive scheme by considering different user priorities and different bit rates as well. In [8], a channel preemption scheme with dynamic priority

T.-L. Sheu (✉) · W.-F. Wei
Department of Electrical Engineering, National Sun Yat-Sen
University, Kaohsiung, Taiwan
e-mail: sheu@ee.nsysu.edu.tw

adjustment was proposed to meet QoS requirements of various types of real-time traffic.

Although Garay and Gopal [9] have proved that finding out a method to determine the minimum number of preempted channels or connections is an NP-Complete problem, Peyravian and Kshemkalyani [10] tried to determine the minimum number of preempted connections by developing two algorithms, the *min_conn* and the *min_bw*. To determine an optimal preemption set, Oliveira et al. [11, 12] used three parameters, the preempted connections, the priorities of preemption, and the preempted bandwidth to define a cost function in MPLS networks. Yao et al. [13] designed a VP (Virtual Partitioning) resource allocation scheme that triggers the channel preemption only when the cellular network becomes congested. In [14, 15], different bandwidth allocation methods are proposed for a differentiated-service-aware network to cope with different channel preemption methods. Cho and Un [16] proposed an M/G/1 channel preemption model given that the service times and the preemption overhead are known. Recently, various channel preemption models were studied in mobile ad hoc networks and optical networks [17–19]. As to the works on vertical handoffs, Janise McNair and Fang Zhu [20] were the first to claim that new vertical handoff techniques are needed to manage user mobility in a 4G multi-network environment. In their later paper [21], a multi-service vertical handoff decision algorithm (MUSE-VDA) based on monetary cost, offered services, network conditions, and user preferences, was proposed and analyzed. Finally, various types of decision strategies for vertical handoffs in heterogeneous wireless networks were fully surveyed in [22]. However, channel preemptions for vertical handoffs were not addressed in these papers [20–22].

In this paper, we consider a heterogeneous wireless network that consists of many WLANs embedded within a cellular network. A mobile node (MN) in this heterogeneous environment may perform vertical handoffs (between a WLAN AP and the cellular base station) frequently. Since in the previous works, none of them have considered channel preemptions in vertical handoffs, performance in terms of handoff-call blocking probabilities may be greatly degraded. Thus, a novel channel preemption model is developed in this paper for vertical handoff users to timely acquire their cellular channels, while the on-going but preempted users are not disrupted.

In the proposed channel preemption model, we assume the coverage area of WLAN is spread evenly and surrounded as a circle co-centered with the cellular network. A newly initiated MN outside the WLAN coverage can preempt the channels occupied by an MN inside the WLAN coverage when the available cellular channels are completely occupied. The channel-preempted MN is forced

to perform vertical handoff to switch its network access to a WLAN. Thus, this proposed channel preemption scheme can effectively reduce the blocking probability while not disrupting any of the existing WLAN connections. For the purpose of performance evaluation, we build a three-dimension Markov chains to analyze the proposed channel preemption mechanism. We derive the equations of move-in and move-out mobility rates based on the node speed and residence times, respectively. Network performance in terms of the number of active WLAN users, the channel utilization and the channel blocking probability of a cellular network, the preemption probability, and the preempted probability of an MN are calculated from the Markov model.

The remainder of this paper is organized as follows. Section 2 describes the heterogeneous channel preemption methods. In Sect. 3, we derive the performance metrics using 3-D Markov chains. Analytical and simulation results are compared in Sect. 4. Finally, we conclude the paper in Sect. 5.

2 Heterogeneous channel preemption scheme

2.1 A WLAN-embedded cellular network

In a WLAN-embedded cellular network, an MN can be in any place as shown in Fig. 1. Due to the mobility of an MN, horizontal (between two WLANs) and vertical handoffs (between a WLAN and the cellular network) are possible in this heterogeneous network environment. Since our main interest in this paper is to study the impact of vertical handoff on the system performance, we assume no

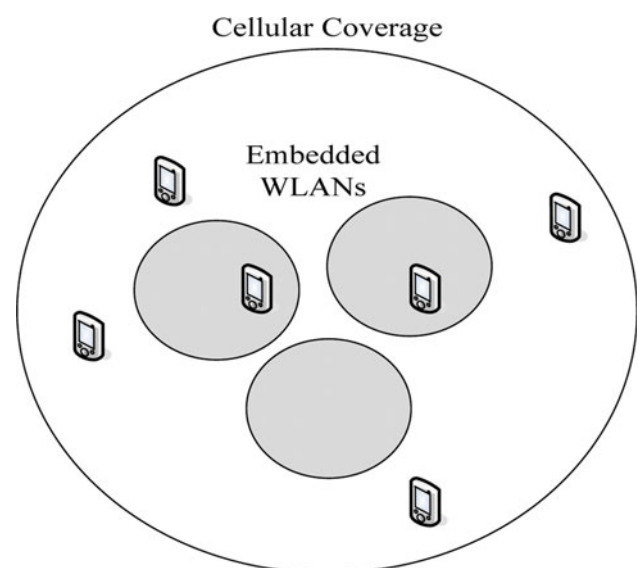


Fig. 1 A WLAN-embedded cellular network

horizontal handoff may occur in our model. Additionally, to avoid unnecessary packet losses and increased packet delay, an MN employing a cellular channel will not perform vertical handoff when it moves into the coverage area of a WLAN. However, vertical handoff could still occur in the following two scenarios.

1. From Cellular to WLAN: While employing a cellular channel (i.e., a cellular user), an MN within the coverage of a WLAN may be compulsory to switch its network access to a WLAN.
2. From WLAN to Cellular: An MN while connecting through a WLAN AP (i.e., a WLAN user) is moving to the outside of WLAN coverage.

Thus, as shown in Fig. 2, there are three types of cellular channels in our model. They are unoccupied (free) channels, occupied but preemptable channels, and occupied but not preemptable channels. The second type represents the channels occupied by an MN within the WLAN coverage and the third type represents the channels occupied by an MN outside the WLAN coverage.

2.2 Channel preemption methods

As mentioned above, vertical handoff could occur in two different scenarios. The first scenario of vertical handoff occurs compulsorily if and only if the following two conditions are met: (1) a newly initiated MN outside the WLAN coverage issues a channel request and found no

free channels, and (2) at least one occupied but preemptable channel exists (i.e., at least one cellular user within the WLAN coverage). In the proposed preemption methods, a newly initiated MN is allowed to perform preemption on a cellular user within the WLAN coverage to reduce the overall channel blocking rate. To prevent from any session disruption, the preempted MN can perform vertical handoff to switch to WLAN access. The second scenario of vertical handoff is relatively straightforward. It occurs when a WLAN user is moving to the outside of WLAN coverage and found no free channels. If one occupied but preemptable channel exists, this mobile MN can perform preemption to reduce the overall handoff blocking rate. Throughout this paper, the first scenario is referred to as preemption-1 and the second scenario as preemption-2.

2.3 Model assumptions

As shown in Fig. 3(a), a WLAN-embedded cellular network in reality may consist of a cellular with radius R and many wireless LANs with radius r_{AP} for each WLAN. Since our main interest is to investigate the performance of vertical handoff with channel preemption under different coverage areas of WLANs, we therefore consider an equivalent topology as shown in Fig. 3(b), where the whole coverage of WLAN is assumed to spread evenly and surrounded as a circle (with radius r) co-centered with the cellular network.

Fig. 2 Three types of cellular channels

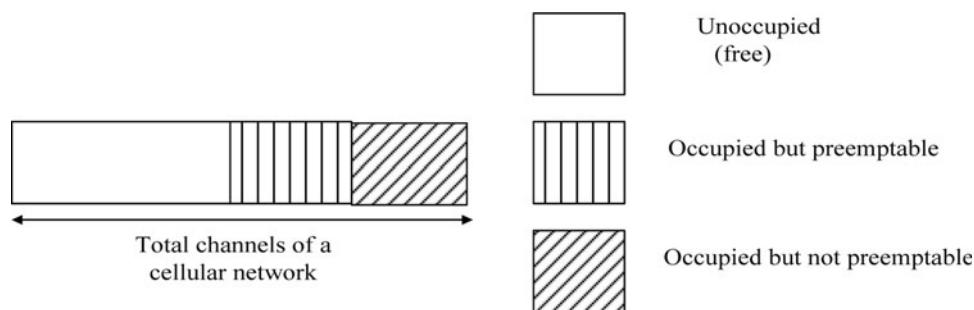
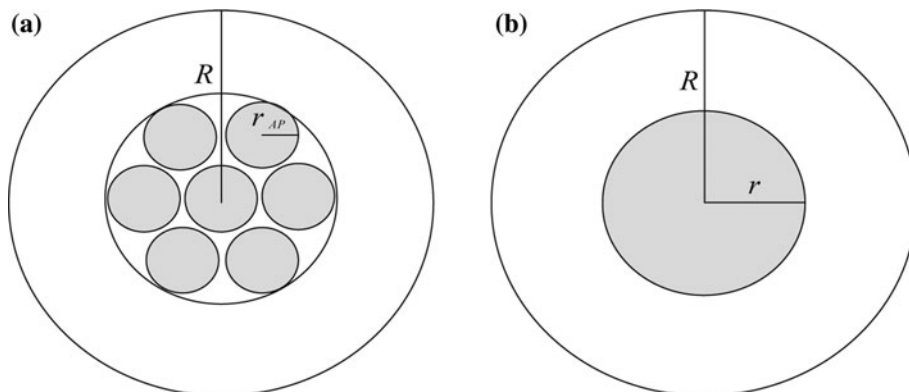


Fig. 3 Equivalent topology of a WLAN-embedded cellular network



In evaluating the blocking and preemption probabilities for a WLAN embedded cellular network, we simply need to know the area ratio between the embedded WLANs and the cellular network. Since we do not consider horizontal handoffs (i.e., handoffs between two WLANs), Fig. 3(a) is considered to be performance-equivalent to a graph where the embedded WLANs are randomly placed inside a cellular network. Additionally, Fig. 3(b) can be considered to be performance-equivalent to Fig. 3(a) due to two reasons; (1) the coverage of embedded WLANs is usually overlapped, and (2) all the MN are assumed to be uniformly distributed across the WLAN and the cellular areas.

To facilitate the set up of mathematical model, we also made the following three assumptions.

1. An MN employs a single channel to become active.
2. An MN within the coverage of WLAN when initiated will choose WLAN as its access point.
3. The channel holding time is independent of the network congestion.

3 Mathematical models

3.1 Channel preemption

As shown in Fig. 4, to build a mathematical model for evaluating the system performance, we design 3-D Markov chains with each state having three parameters. They are:

- i* The number of MN outside the WLAN coverage and these MN are employing cellular channels
- j* The number of MN within the WLAN coverage and these MN are employing cellular channels
- k* The number of MN within the WLAN coverage and these MN are connecting through WLAN AP

If we let *N* denote the total number of MN (including idle and active nodes) and *C* represent the cellular capacity (i.e., the total number of cellular channels), then we have $i + j \leq C$ and $i + j + k \leq N$.

In the Markov model, we assume the MN arrival rate is exponentially distributed with a mean λ . In other words, an idle MN will become active every $\frac{1}{\lambda}$ s. Similarly, the MN departure rate is exponentially distributed with a mean μ . This implies that an MN goes to idle state after becoming active for $\frac{1}{\mu}$ s. The state transition rates of the MN arrival

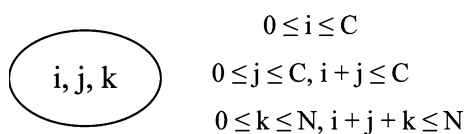


Fig. 4 Definition of a Markovian state

and departure process in the Markov chains are listed from Eq. 1–5, respectively. Note that in these equations, *R* (current state | next state) is defined as a transition rate from the current state to the next state. For simplicity, we also use *a* to represent the area ratio between the WLAN coverage and the cellular coverage. Thus, we have $a = \frac{r^2}{R^2}$.. Note that *a* will be referred to as “the WLAN coverage ratio” throughout the paper.

MN arrival process:

$$R(i, j, k | i + 1, j, k) = [N - (i + j + k)] \times \lambda \times (1 - a), \quad (1)$$

if $i + j < C, i + j + k < N;$

$$R(i, j, k | i, j, k + 1) = [N - (i + j + k)] \times \lambda \times a, \quad (2)$$

if $i + j + k < N;$

MN departure process:

$$R(i, j, k | i - 1, j, k) = i \times \mu, \quad \text{if } i \geq 1; \quad (3)$$

$$R(i, j, k | i, j - 1, k) = j \times \mu, \quad \text{if } j \geq 1; \quad (4)$$

$$R(i, j, k | i, j, k - 1) = k \times \mu, \quad \text{if } k \geq 1. \quad (5)$$

As described in Sect. 2.2, channel preemption could occur in two different scenarios. They are referred to as Preemption-1 and Preemption-2, respectively. Thus, the transition rates of these two preemptions can be expressed respectively as below.

Preemption-1:

$$R(i, j, k | i + 1, j - 1, k + 1) = [N - (i + j + k)] \times \lambda \times (1 - a), \quad (6)$$

if $i + j = C, j > 0;$

Preemption-2:

$$R(i, j, k | i + 1, j - 1, k) = j \times \zeta_{out} + k \times \zeta_{out}, \quad (7)$$

if $i + j = C, j > 0.$

In Eq. 7, we let ζ_{out} represent the reciprocal of residence time that an MN might stay within the WLAN coverage. Hence, $j \times \zeta_{out}$ and $k \times \zeta_{out}$, respectively, denote how many cellular users and how many WLAN users per unit time that may move to the outside of WLAN coverage. The role of ζ_{out} will become clear and it will be discussed in more detail in the next section.

3.2 Mobility and residence times

The mobility rates of MN within the WLAN coverage can be discussed from two different aspects, the move-in and the move-out, which are directly related to the node speed and the area ratio of the WLAN coverage within the cellular network. As shown in Fig. 5, we use the circle with radius *r* to represent the WLAN coverage and the circle with radius *R* for the cellular coverage. For an MN with speed *v* to move out the WLAN coverage in time *t*, its starting position must be inside the dark shaded area (with

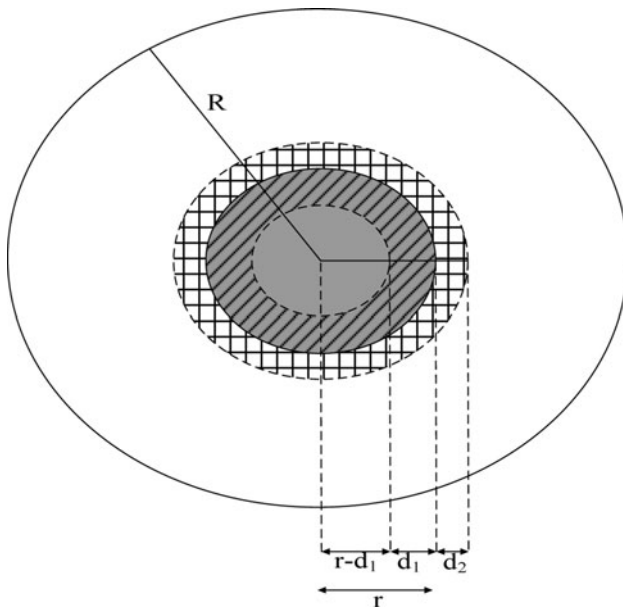


Fig. 5 MN mobility in a WLAN-embedded cellular network

oblique lines) between two circles with radius $r - d_1$ and r , respectively. Therefore, we have $d_1 = v \times t$. If we let N_N denote the number of MN (including WLAN and cellular users) within the WLAN coverage, then the maximum number of MN that may move out to the WLAN coverage in time t can be expressed as

$$N_N \times \frac{r^2 - (r - d_1)^2}{r^2}. \tag{8}$$

Thus, the maximum number of MN that may move out to the WLAN coverage per unit time becomes

$$N_N \times \frac{r^2 - (r - d_1)^2}{r^2 \times t}. \tag{9}$$

Let ζ_{out} represent the reciprocal of residence time that an MN might stay within the WLAN coverage. Thus, $k \times \zeta_{out}$ denotes the move-out mobility rate (users/s) of WLAN users. From Eq. 9, we have,

$$k \times \zeta_{out} = N_N \times \frac{r^2 - (r - d_1)^2}{r^2 \times t} \times \frac{k}{N_N}. \tag{10}$$

Thus, the reciprocal of residence time that an MN might stay within the WLAN coverage is expressed as

$$\zeta_{out} = \frac{r^2 - (r - d_1)^2}{r^2 \times t}. \tag{11}$$

Similarly, we can derive the maximum number of cellular users that may move into the coverage of WLAN per unit time (i.e., the move-in mobility rate of cellular users, or $i \times \zeta_{in}$). As shown in Fig. 5, since MN is assumed to be uniformly distributed across the WLAN and the cellular

areas, the light shaded area (with lattices) must be equal to the dark shaded area (with oblique lines). That is,

$$r^2 - (r - d_1)^2 = (r + d_2)^2 - r^2. \tag{12}$$

From the equality of 12, we can solve for d_2 . That is,

$$d_2 = \frac{\sqrt{4r^2 + 4(2rd_1 + d_1^2)} - 2r}{2}. \tag{13}$$

When a cellular user moves into the WLAN coverage, there is only one state change in the Markov chains as shown in Eq. 14, where ζ_{in} represents the reciprocal of residence time that an MN might stay outside the WLAN coverage.

$$R(i, j, k | i - 1, j + 1, k) = i \times \zeta_{in}. \tag{14}$$

Using the similar method for deriving ζ_{out} , we can derive ζ_{in} as shown in Eq. 15.

$$\zeta_{in} = \frac{(r + d_2)^2 - r^2}{(R^2 - r^2) \times t}. \tag{15}$$

3.3 The 3-D Markov model

Figure 6 shows all the transition of state (i, j, k) in the 3-D Markov model. The corresponding transition rates are listed in Table 1, where we classify the rates into two categories. For any transition that flows into the state (i, j, k) is defined in the Arrival process, and for the transition that flows out from the state (i, j, k) is defined in the departure process. A general 3-D Markov model is illustrated in Fig. 7. As shown in the figure, the model consists of $(N - C + 1)$ isosceles triangles with all equal side length C (for $0 \leq k \leq N - C$) and C isosceles triangles with unequal side length descending from $C - 1$ to 0 (for $N - C < k \leq N$). Notice that at the first plane for $k = 0$, there exists no WLAN users and the maximum number of $(i + j)$ equals C (i.e., the upper limit of channel capacity). From Fig. 7, we can calculate the total number of Markov states (M) as shown in Eq. 16.

$$M = \sum_{i=1}^{C+1} i \times (N + 2 - i). \tag{16}$$

By applying the equilibrium point analysis (EPA) to the Markov model, for each state we can find a flow equilibrium equation. By assuming that the sum of all the state probabilities equals one, we can solve the steady-state probability of the Markov model.

3.4 Performance metrics

Based on the derived steady-state probabilities of the Markov model, we are interested in evaluating the

Fig. 6 State transition of (i, j, k) in the 3-D Markov chains

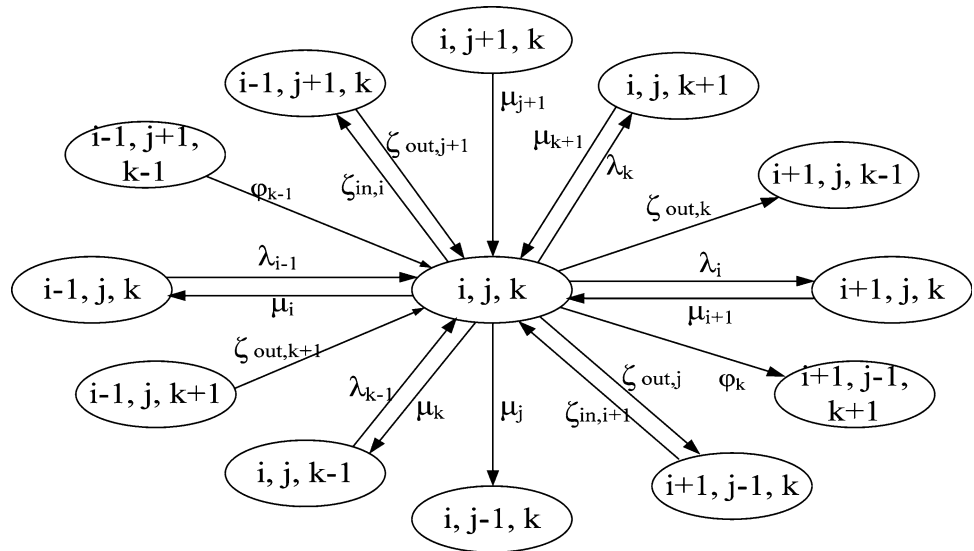


Table 1 State transition rates

Arrival process	Departure process
$\lambda_{i-1} = [N - (i - 1 + j + k)] \times \lambda \times (1 - a)$	$\lambda_i = [N - (i + j + k)] \times \lambda \times (1 - a)$
$\lambda_{k-1} = [N - (i + j + k - 1)] \times \lambda \times a$	$\lambda_k = [N - (i + j + k)] \times \lambda \times a$
$\mu_{i+1} = (i + 1) \times \mu$	$\mu_i = i \times \mu$
$\mu_{j+1} = (j + 1) \times \mu$	$\mu_j = j \times \mu$
$\mu_{k+1} = (k + 1) \times \mu$	$\mu_k = k \times \mu$
$\zeta_{out,j+1} = \begin{cases} (j + 1) \times \zeta_{out}, & \text{if } i + j + 1 < C \\ (j + 1) \times \zeta_{out} + k \times \zeta_{out}, & \text{if } i + j + 1 = C \end{cases}$	$\zeta_{out,j} = \begin{cases} j \times \zeta_{out}, & \text{if } i + j < C \\ j \times \zeta_{out} + k \times \zeta_{out}, & \text{if } i + j = C \end{cases}$
$\zeta_{in,i+1} = (i + 1) \times \zeta_{in}$	$\zeta_{in,i} = i \times \zeta_{in}$
$\zeta_{out,k+1} = \begin{cases} (k + 1) \times \zeta_{out}, & \text{if } i - 1 + j < C \\ 0, & \text{if } i - 1 + j = C \end{cases}$	$\zeta_{out,k} = \begin{cases} k \times \zeta_{out}, & \text{if } i + j < C \\ 0, & \text{if } i + j = C \end{cases}$
$\varphi_{k-1} = [N - (i + j + k - 1)] \times \lambda \times (1 - a), \quad \text{if } i + j = C \text{ and } j > 0$	$\varphi_k = [N - (i + j + k)] \times \lambda \times (1 - a), \quad \text{if } i + j = C \text{ and } j > 0$

performance metrics which include the average number of WLAN users (N_{WLAN}), the average channel utilization (CU), the channel blocking probability (P_{CB}), the pre-emption probability (P_{PREN}), and the preempted probability (P_{PRED}). These metrics are derived one by one as listed below.

1. Average number of WLAN users (N_{WLAN}): By multiplying the number of WLAN users to the corresponding steady-state probabilities, we can calculate N_{WLAN} as shown in Eq. 17.

$$N_{WLAN} = \sum_{k=0}^{N-C} \sum_{j=0}^C \sum_{i=0}^{C-j} k \times p(i, j, k) + \sum_{k=N-C+1}^N \sum_{j=0}^{N-k} \sum_{i=0}^{N-k-j} k \times p(i, j, k) \quad (17)$$

2. Average Channel Utilization (ACU): Channel utilization is defined as a ratio between the occupied channels and the total available channels. By multiplying the ratio to the corresponding steady-state probabilities, we can compute the ACU as shown in Eq. 18.

$$ACU = \sum_{k=0}^{N-C} \sum_{j=0}^C \sum_{i=0}^{C-j} \frac{(i+j)}{C} \times p(i, j, k) + \sum_{k=N-C+1}^N \sum_{j=0}^{N-k} \sum_{i=0}^{N-k-j} \frac{(i+j)}{C} \times p(i, j, k). \quad (18)$$

3. Channel Blocking Probability (P_{CB}): P_{CB} is defined as the probability that a channel request issued by an MN is rejected. When the available channels and the

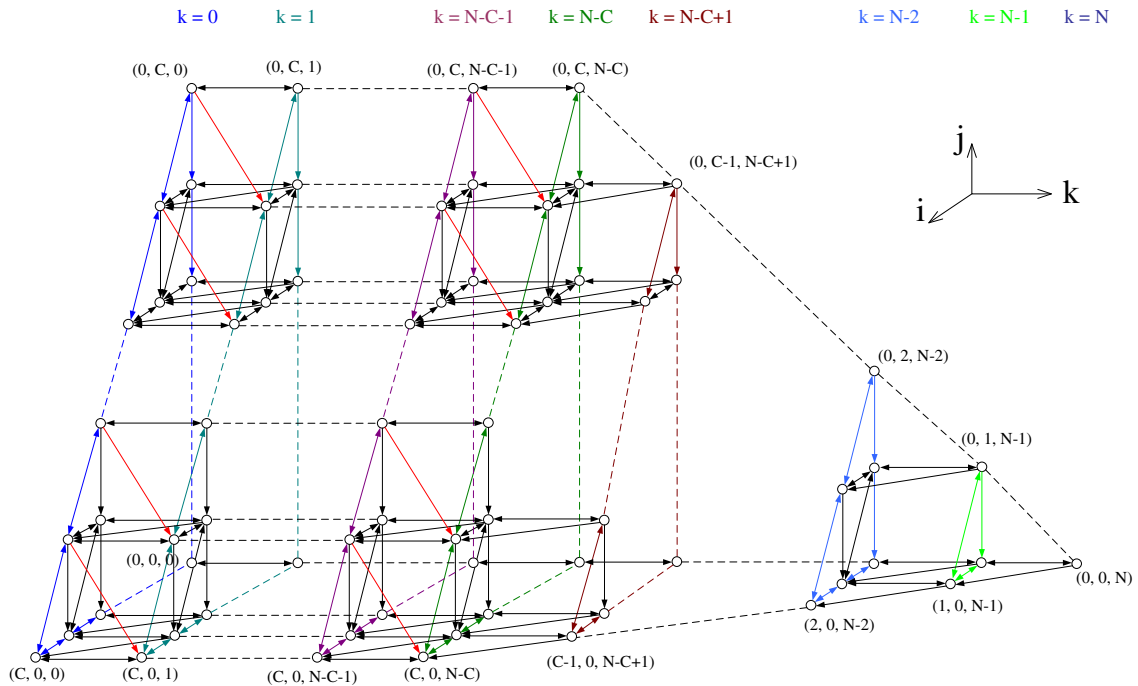


Fig. 7 A general 3-D Markov model of channel preemption

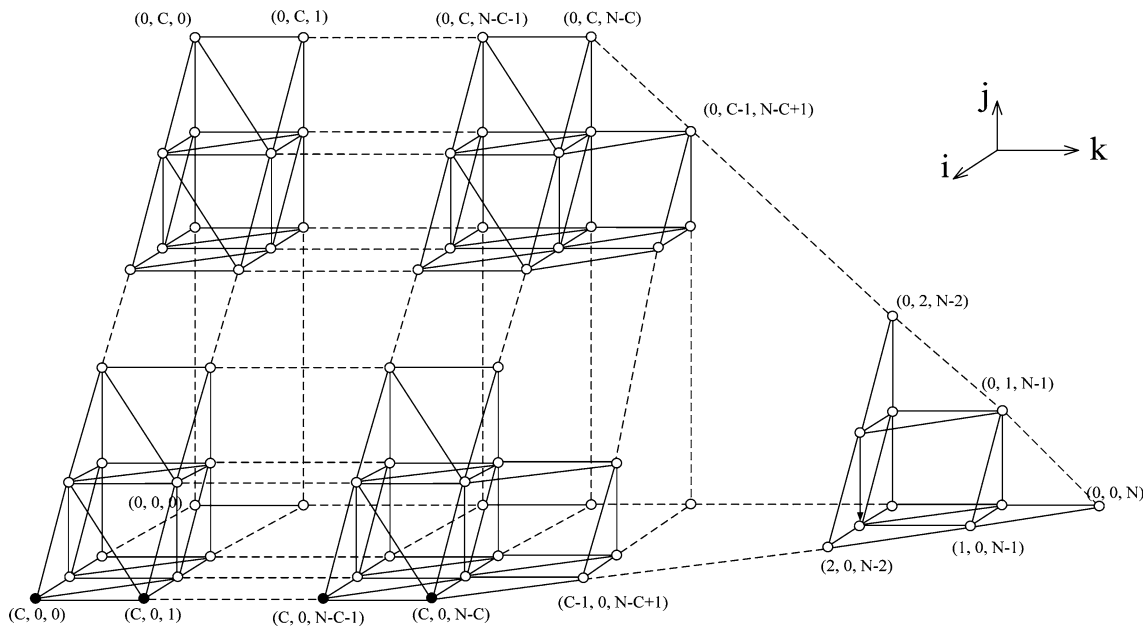


Fig. 8 Channel blocking probability (P_{CB})

occupied but preemptable channels are all zero, a newly initiated MN outside the WLAN coverage and a handoff MN moving away from the WLAN coverage are all rejected. As shown in Fig. 8, the white dots represent the states that channel requests can be granted and the black dots denote the states that channel requests are rejected. Thus, by summing up all the steady-state probabilities of black dots, we can derive P_{CB} in Eq. 19.

$$P_{CB} = \sum_{k=0}^{N-C} p(C, 0, k). \tag{19}$$

4. Preemption Probability (P_{PREN}): P_{PREN} is defined as the probability that a newly initiated MN outside the WLAN coverage or a handoff MN moving away from the WLAN coverage may preempt an occupied but preemptable channel if no free channels are available.

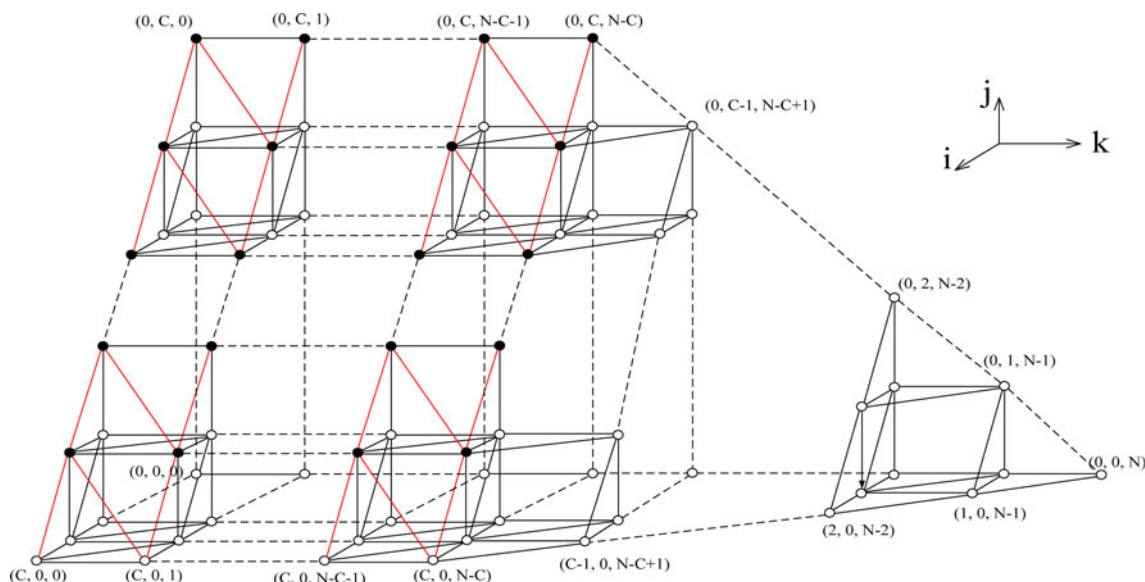


Fig. 9 Preemption probability (P_{PREN})

As shown in Fig. 9, the black dots represent the states that channel preemption can occur. By summing up all the steady-state probabilities of black dots, we can compute P_{PREN} as shown in Eq. 20.

$$P_{\text{PREN}} = \sum_{k=0}^{N-C} \sum_{i=0}^{C-1} p(i, C-i, k). \tag{20}$$

5. Preempted Probability (P_{PRED}): P_{PRED} is defined as the probability that a cellular user inside the WLAN coverage is preempted. Based on our definition in Sect. 2.1, an occupied but preemptable channel is the channel employed by an MN moving into the WLAN coverage. As shown in Fig. 10, the black dots represent the states that an MN employing a cellular channel resides in the WLAN coverage. Yet, from Fig. 9, we know the preemption occurs when a newly initiated MN outside the WLAN coverage or a handoff MN moving away from the WLAN coverage issues a channel request and it got rejected because of no free channels. Thus, P_{PRED} is a conditional probability as shown in Eq. 21. The numerator represents the state probabilities of channel requests and the denominator represents the state probabilities of occupied but preemptable channels.

4 Analytical results versus simulation

In this section, we first use the MATLAB tool to calculate the analytical results based on Eqs. 17–21, and then we perform a simulation on NS-2 to validate the analytical results.

4.1 Simulation model

In the NS-2 simulation model, a platform with a cellular radius being 6 km is assumed. Mobile nodes (MN) are uniformly distributed in the platform with mean node speed ranged from 10 to 50 km/h. The moving directions of MN are uniformly distributed in $[0, 2\pi]$ without changing direction during session duration. MN generation rate (or arrival rate) and departure rate in a unit area are assumed to be Poisson process. The session duration period of MN is exponentially distributed with mean 100 s. The target WLAN simulated in the NS-2 model is IEEE 802.11 g with 54-Mbps bit rate. The data rate of a mobile user is assumed to be 1 Mbps and average packet length is 1024 Kbytes. Other parameters used in the simulation and analytical computations are listed in Table 2. All the parameter settings in Table 2 are referred to the characteristics of multimedia sessions. Each simulation runs for 30,000 s and

$$P_{\text{PRED}} = \frac{\sum_{k=0}^{N-C} \sum_{i=0}^{C-1} \frac{1}{C-i} \times p(i, C-i, k)}{\sum_{k=0}^{N-C} \sum_{j=1}^C \sum_{i=0}^{C-j} p(i, j, k) + \sum_{k=N-C+1}^N \sum_{j=1}^{N-k} \sum_{i=0}^{N-k-j} p(i, j, k)}. \tag{21}$$

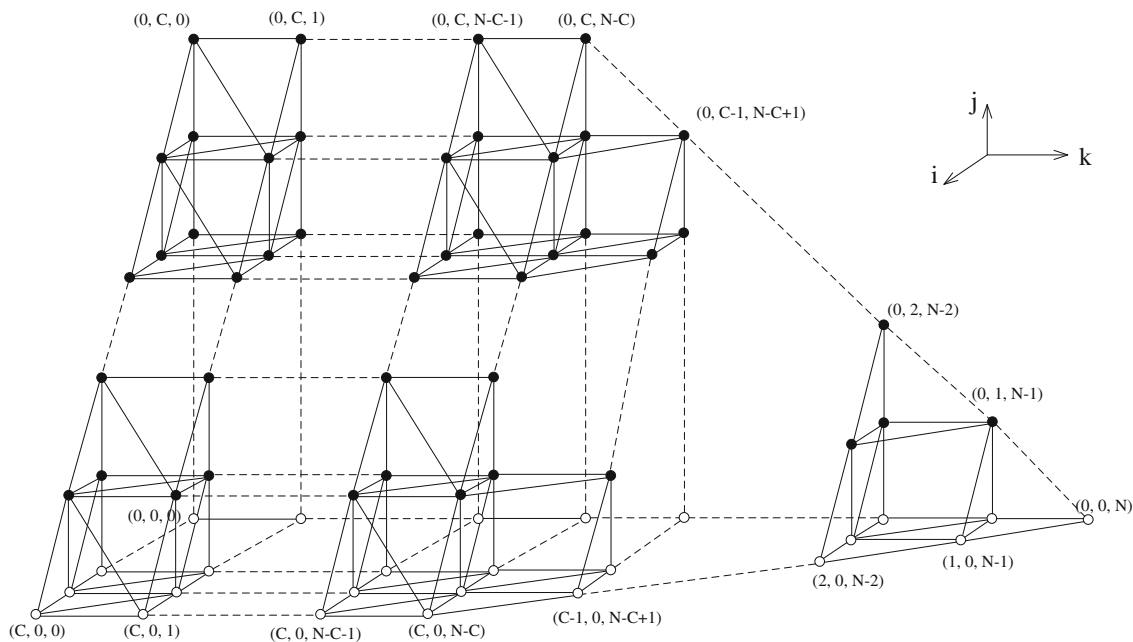


Fig. 10 Preempted probability (P_{PRED})

Table 2 Parameter settings in the performance analysis

Parameters and notations	Settings
N (The number of MN)	40
C (The total number of cellular channels)	20
R (Cellular radius)	6 km
a (The WLAN coverage ratio)	0.1–0.9
v (Mean node speed)	10–50 km/h
$k \times \zeta_{\text{out}}$ (Move-out mobility rate of WLAN users)	0.01 users/s
$i \times \zeta_{\text{in}}$ (Move-in mobility rate of cellular users)	0.01 users/s
Bit rate per mobile user	1 Mbps
Average packet length	1024 bytes
λ (MN arrival rate)	0.01–0.03
μ (MN departure rate)	0.02

all the simulation results are averaged of up to 10 repeated runs.

4.2 Analytical and simulation results

Due to the huge number of Markov states that can be generated from Eq. 16, we consider 40 mobile nodes evenly distributed in a cellular network with 20 channels. By fixing the node speed to 50 km/h, Fig. 11 shows the average number of WLAN users (N_{WLAN}) versus the WLAN coverage ratio. Increasing the ratio can increase N_{WLAN} accordingly. We also observe that when the ratio is relatively small (0.1 or 0.2), the differences in N_{WLAN} become insignificant. In general, simulation results are lower than the analytical data. One explanation for this is

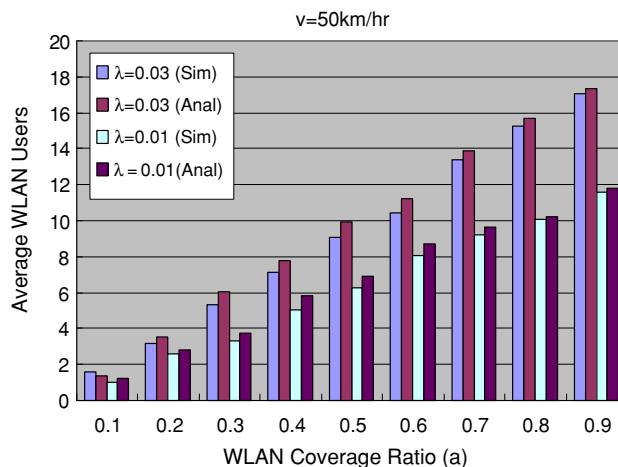


Fig. 11 Average WLAN users versus the WLAN coverage ratio

that a system realized through simulation can capture more network characteristics than a simplified mathematical model. For instance, the handoff delay, may play an important role in the number of WLAN users, is ignored in the analytical model. Nevertheless, it is noticed that the analytical results are getting closer to the simulation as the WLAN coverage ratio increases. This interesting phenomenon reveals that our analytical model can predict the performance more accurately when the total WLAN coverage is close to the cellular area.

By fixing the WLAN coverage ratio to 0.5, as shown in Fig. 12, the increase of node speed (from 10 to 50 km/h) can gradually reduce the average number of WLAN users. Again, the analytical results are slightly higher than the

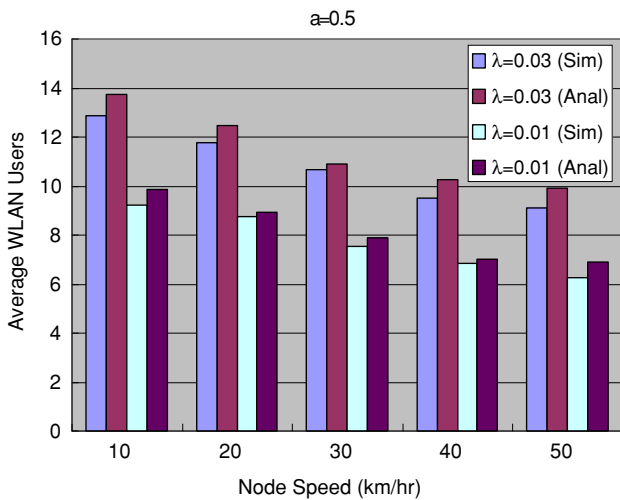


Fig. 12 Average WLAN users versus node speed

simulation data no matter which MN arrival rate is (0.01 or 0.03). The increase of node speed can increase the users of moving into the WLAN coverage per unit time, but it also increases the users of moving out. Hence, the real reason for the decrease of N_{WLAN} as the node speed increases is because in our model a cellular user does not perform vertical handoff when he moves into the WLAN coverage; he may become a WLAN user only when channel preemption is invoked.

To further study the impact of the proposed preemption methods on the WLAN performance, Fig. 13 shows the average packet delay versus the WLAN coverage ratio. As the ratio increases from 0.1 to 0.9, we observe that average packet delay consumed in the WLAN increases very quickly when arrival rate = 0.03, yet it dose not vary too much when arrival rate = 0.01. This is because in the former case WLAN users, as can be observed from Fig. 11, increases from 1.8 to 17.5, which naturally increases the

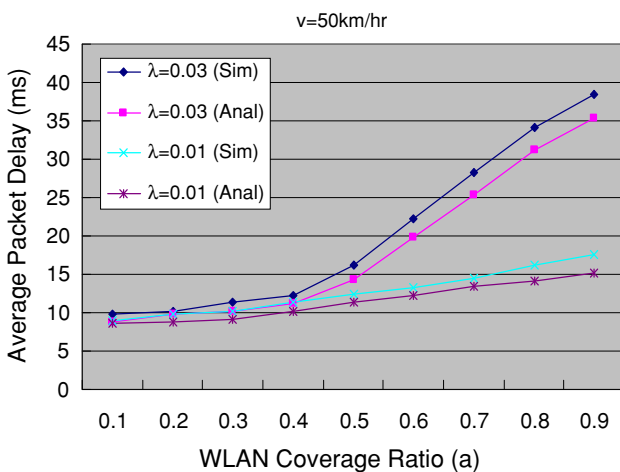


Fig. 13 Average packet delay in WLAN

back-off time exponentially after every time of collision. Another observation is that the analytical results of average packet delay, derived directly from Eq. 17 and Little’s law, do not greatly deviate from the simulation results even when the arrival rate is large ($\lambda = 0.03$).

Figure 14 shows the average channel utilization (ACU) versus the WLAN coverage ratio. As can be seen, both analytical and simulation results show that ACU gradually decreases when the WLAN coverage ratio is increased from 0.1 to 0.9. The reason for this decrease is quite straightforward; since MN is assumed to be uniformly distributed over the WLAN and the cellular areas, increasing the WLAN coverage ratio will largely increase the number of WLAN users, which naturally decreases the channel utilization. From Fig. 14, we also observe that different MN arrival rates may play an important factor on ACU only when the WLAN coverage ratio is small. When the coverage ratio is increased to above 0.7, the effect of different MN arrival rates (0.03 vs. 0.01) on ACU becomes smaller due to the quickly decreased cellular users.

Figure 15 shows the channel blocking probability (P_{CB}) versus the WLAN coverage ratio. It is observed that P_{CB} is drastically decreased to zero as the ratio is increased from 0.1 to 0.7. This is because when the ratio equals 0.7, the number of cellular users is reduced to become less than the available cellular channels. Thus, a larger MN arrival rate ($\lambda = 0.03$) may have more impact on P_{CB} than a smaller arrival rate ($\lambda = 0.01$) only when the ratio of WLAN coverage is small. As shown in Fig. 16, it is very interesting to observe that the probability of preemption (P_{PREN}) increases and then decreases drastically as the

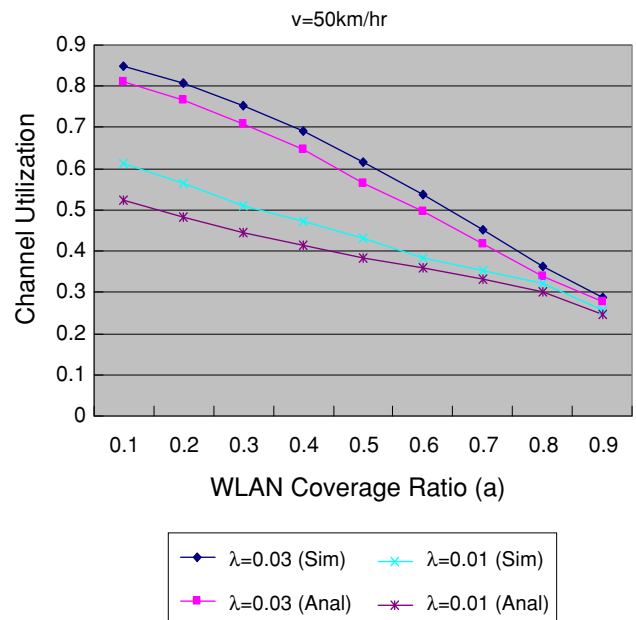


Fig. 14 Average channel utilization versus the WLAN coverage ratio

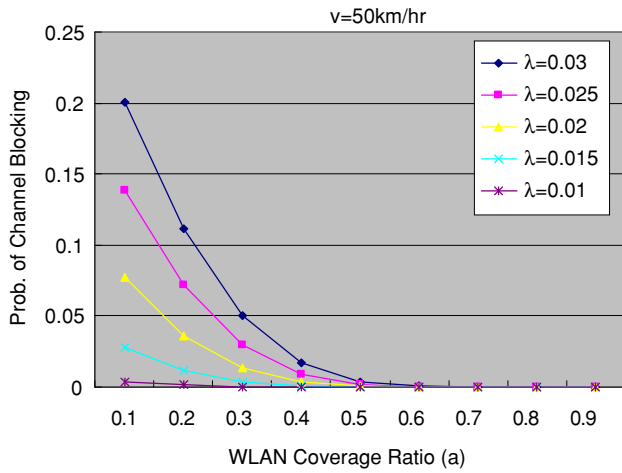


Fig. 15 Channel blocking probability versus the WLAN coverage ratio

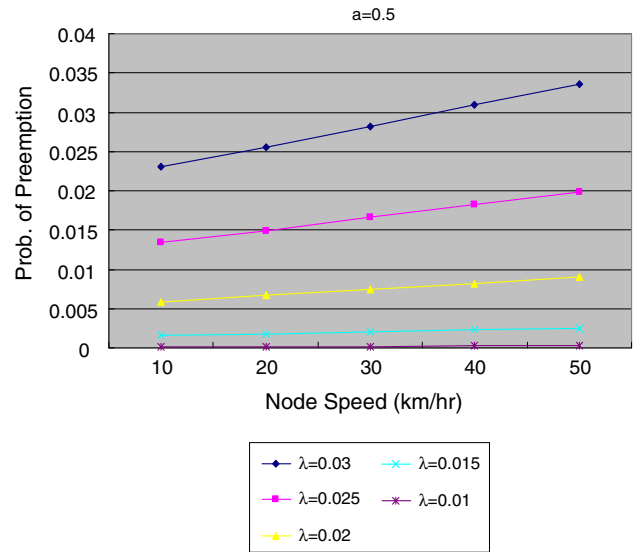


Fig. 17 Preemption probability versus node speed

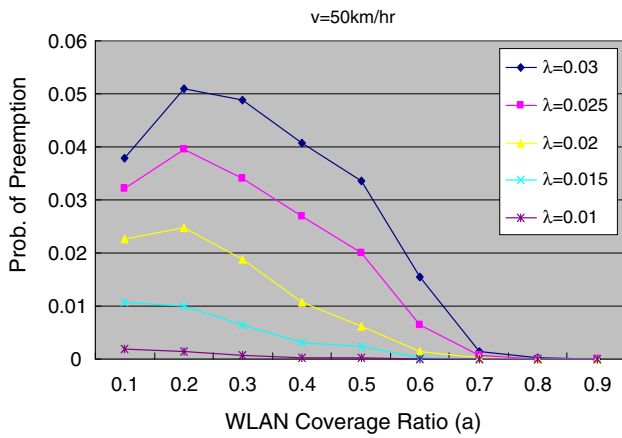


Fig. 16 Preemption probability versus the WLAN coverage ratio

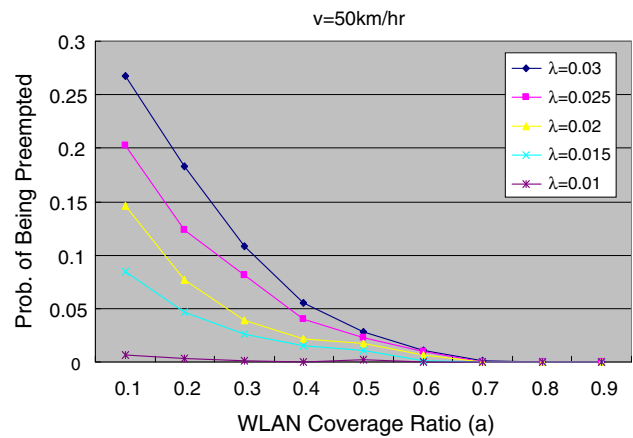


Fig. 18 Preempted probability versus the WLAN coverage ratio

increase of the WLAN coverage ratio. This increasing first and then decreasing phenomenon is more significant if the MN arrival rate is large (i.e., when $\lambda \geq 0.02$). As we know, the occurrence of preemption must meet two conditions: (1) no free channels exist when a request is issued, and (2) at least one occupied and preemptable channel exists. The first condition implies that P_{PREN} is a descending function of the number of MN which may issue preemption requests, while the second condition implies that P_{PREN} is an ascending function of the number of preemptable channels. In other words, when the WLAN coverage ratio is small, the first condition dominates which makes P_{PREN} to increase quickly. As the ratio is increased to exceed 0.2, the second condition takes turns to dominate P_{PREN} , which therefore drives P_{PREN} to fast decline to near zero.

Figure 17 shows the relationship between the preemption probability (P_{PREN}) and the node speed. By fixing the WLAN coverage ratio to 0.5, we can observe that even for a larger MN arrival rate (e.g., $\lambda = 0.03$) the increase of

node speed from 10 to 50 km/h only slightly increases the preemption probability from near zero to 0.033. Thus, we can claim that the variation of node speed does not have very significant impact on the preemption probability, which is good for a wireless and mobile environment.

Based on Eq. 21, Fig. 18 shows the relationship between the preempted probability (P_{PREN}) and the ratio of WLAN coverage. Remember P_{PREN} is defined as the probability that a cellular user within the WLAN coverage is preempted. As can be seen, P_{PREN} decreases very quickly as the ratio increases. The reasons can be explained from three aspects; as the ratio is increased, (1) the probability of MN moving into the WLAN coverage is increased, which in turns increases the number of preemptable candidates, (2) it is becoming less possible for an MN to move out the WLAN coverage, and (3) the number of MN that may issue a channel request becomes smaller. The first aspect reduces the possibility of channels being

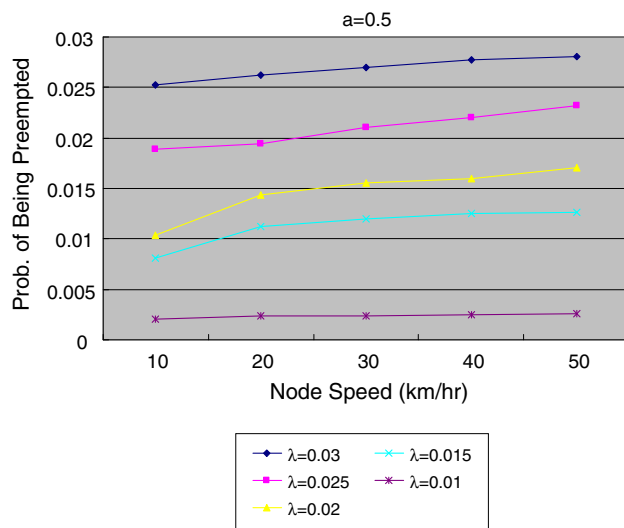


Fig. 19 Preempted probability versus node speed

preempted, while the second and the third aspects reduce the possibility of channel preemption.

Finally, the preempted probability as a function of node speed is shown in Fig. 19. Again, even for a larger MN arrival rate (e.g., $\lambda = 0.03$), P_{PRED} increases almost unnoticeably as the node speed increases from 10 to 50 km/h. This is because when the WLAN coverage ratio is fixed to 0.5, the number of preemptable candidates does not increase very largely along with the increase of node speed.

5 Conclusions

In this paper, we have presented a channel preemption model for vertical handoff in a WLAN-embedded cellular network. The major creativity thought of this paper is right in that a newly initiated MN outside the WLAN coverage can preempt the channels occupied by an MN inside the WLAN coverage when the cellular channels are completely used up. The channel preempted MN can still maintain its connection through vertical handoff to WLAN AP. Thus, with this preemption scheme, channel blocking probability can be substantially reduced while not disrupting any of the existing connections within WLANs.

For the purpose of performance evaluation, we built a three-dimension Markov chains to analyze the proposed channel preemption methods, and then followed by a simulation on NS-2 to validate the analytical results. In the analytical model, we derived the equations of move-in and move-out mobility rates based on the node speed and their residence times, respectively. From the analytical and simulation results, we observed an interesting and significant phenomenon; the probability of preemption (P_{PREN})

increases initially and then decreases dramatically as the increase of the WLAN coverage ratio. We also revealed that there are three major factors that could drive the preempted probability (P_{PRED}) to decrease very quickly as the ratio increases. Finally, we demonstrated that the variation of node speed does not play a significant role in the preemption and the preempted probabilities. One of our future works on this paper is to build a more general mathematical model by relaxing the assumptions and restrictions on the WLAN coverage.

References

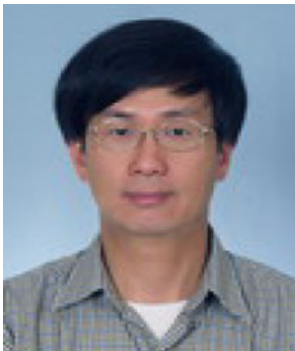
- Chen, W.-Y. & Wu, J.-L. C. (2005). Performance analysis of radio resource allocation for multimedia traffic in cellular networks. In *19th International conference on advanced information networking and applications* (Vol. 1, pp. 432–437).
- Ahmad, I., Kamruzzaman, J., & Aswathanarayanan, S. (2005). An improved preemption policy for higher user satisfaction. In *19th International conference on advanced information networking and applications* (Vol. 1, pp. 749–754).
- Das, S. K., Sen, S. K., Basu, K., & Lin, H. (2003). A framework for bandwidth degradation and call admission control schemes for multiclass traffic in next-generation wireless networks. *IEEE Journal on Selected Areas in Communications*, 21(10), 1790–1802.
- Oliver, Y., Saric, E., & Li, A. (2005). Adaptive prioritized admission over CDMA. *IEEE Wireless Communications and Networking Conference*, 2, 1260–1265.
- Yu, O., Saric, E., & Li, A. (2006). Fairly adjusted multimode dynamic guard bandwidth admission control over CDMA systems. *IEEE Journal on Selected Areas in Communications*, 24(3), 579–592.
- Kim, S., & Varshney, P. K. (2003). Adaptive load balancing with preemption for multimedia cellular networks. *IEEE Wireless Communications and Networking Conference*, 3, 1680–1684.
- Kim, S., & Varshney, P. K. (2004). An integrated adaptive bandwidth-management framework for QoS-sensitive multimedia cellular networks. *IEEE Transactions on Vehicular Technology*, 53(3), 835–846.
- Do, M.-S., Park, Y., & Lee, J.-Y. (2002). Channel assignment with QoS guarantees for a multiclass multicode CDMA system. *IEEE Transactions on Vehicular Technology*, 51(5), 935–948.
- Garay, J. A., & Gopal, I. S. (1992). Call preemption in communication networks. In *11th Annual joint conference of the IEEE computer and communications societies, INFOCOM '92* (Vol. 3, pp. 1043–1050).
- Peyravian, M., & Kshemkalyani, A. D. (1997). Connection preemption: Issues, algorithms, and a simulation study. In *16th Annual joint conference of the IEEE computer and communications societies, INFOCOM '97* (Vol. 1, pp. 143–151).
- de Oliveira, J. C., Scoglio, C., Akyildiz, I. F., & Uhl, G. (2002). A new preemption policy for DiffServ-aware traffic engineering to minimize rerouting. In *Twenty-First Annual joint conference of the IEEE computer and communications societies, INFOCOM '02* (Vol. 2, pp. 695–704).
- de Oliveira, J. C., Scoglio, C., Akyildiz, I. F., & Uhl, G. (2004). New preemption policies for DiffServ-aware traffic engineering to minimize rerouting in MPLS networks. *IEEE/ACM Transactions on Networking*, 12(4), 733–745.

13. Yao, J., Mark, J. W., Wong, T. C., Chew, Y. H., Lye, K. M., & Chua, K.-C. (2004). Virtual partitioning resource allocation for multiclass traffic in cellular systems with QoS constraints. *IEEE Transactions on Vehicular Technology*, 53(3), 847–864.
14. Shan, T., Dam, H., & Yang, O. (2002). Bandwidth allocation and preemption for supporting differentiated-service-aware traffic engineering in multi-service networks. *IEEE International Conference on Communications*, 2, 1305–1309.
15. Shan, T., & Yang, O. W. W. (2005). Bandwidth preemption algorithms for differentiated service aware traffic engineering. *IEEE Global Telecommunications Conference*, 1, 535–539.
16. Cho, Y. Z., & Un, C. K. (1993). Analysis of the M/G/1 queue under a combined preemptive/nonpreemptive priority discipline. *IEEE Transactions on Communications*, 41(1), 132–141.
17. Klinkowski, M., Careglio, D., Morato, D., & Sole-Pareta, J. (2006). Effective burst preemption in OBS network. *Workshop on High Performance Switching and Routing*, 371–377.
18. Phuritakul, J., Yusheng, J., & Zhang, Y. (2006). Blocking probability of a preemption-based bandwidth-allocation scheme for service differentiation in OBS networks. *Journal of Lightwave Technology*, 24(8), 2986–2993.
19. Tan, C. W., Mohan, G., & Lui, J. C.-S. (2006). Achieving multi-class service differentiation in WDM optical burst switching networks: A probabilistic preemptive burst segmentation scheme. *IEEE Journal on Selected Areas in Communications*, 24(12), 106–119.
20. McNair, J., & Zhu, F. (2004). Vertical handoffs in fourth-generation multi-network environments. *IEEE Wireless Communications*, 11, 10–15.
21. Zhu, F., & McNair, J. (2006). Multiservice vertical handoff decision algorithms. *EURASIP Journal on Wireless Communications and Networking*, 2006, 1–13. Article ID 25861.
22. Kassar, M., Kervella, B., & Pujolle, G. (2008). An overview of vertical handoff decision strategies in heterogeneous wireless networks. *Computer Communications*, 31, 2607–2620. (Online).



Wei-Feng Wei received the B.S. degree from the Department of Electrical Engineering, Tatung University, Taipei, Taiwan, in 2005, and the M.S. degree from the Department of Electrical Engineering, National Sun Yat-Sen University, Kaohsiung, Taiwan, in 2007. His research interests are in the area of wireless and mobile networks, with emphasis on vertical handoff schemes in WLAN-embedded cellular systems.

Author Biographies



Tsang-Ling Sheu received the Ph.D. degree in Computer Engineering from the Department of Electrical and Computer Engineering, Penn State University, University Park, Pennsylvania, USA, in 1989. From September 1989 to July 1995, he worked with IBM Corporation at Research Triangle Park, North Carolina, USA. In August 1995, he became an associate professor, and was promoted to full professor in

January 2006 at the Department of Electrical Engineering, National Sun Yat-Sen University, Kaohsiung, Taiwan. His research interests include wireless mobile networks and multimedia networking. He was the recipient of the 1990 IBM Outstanding Paper Award. Dr. Sheu is a senior member of the IEEE, and the IEEE Communications Society.